

CALIBRATION AND TESTING OF SIMULATION PARAMETERS FOR RAPESEED BLANKET SEEDLING SHEETS BASED ON DISCRETE ELEMENT METHOD

基于离散元法的油菜毯状苗的苗片仿真参数标定与测试

Qing TANG^{1,2)}, Jing LUO¹⁾, Minghui HUANG²⁾, Jun WU¹⁾, Lan JIANG^{*1)}, Zhewen SONG²⁾, Wei SHI²⁾, Yang WU²⁾

¹⁾ Nanjing Institute of Agricultural Mechanization, Ministry of Agriculture and Rural Affairs of China, Nanjing 210014 / China;

²⁾ Sinomach Changlin Company Limited, Changzhou 213002 / China;

Corresponding author: Lan JIANG

Tel: +86.17372778343; E-mail: jianglan@caas.cn

DOI: <https://doi.org/10.35633/inmateh-76-65>

Keywords: discrete element simulation, maximum shear force, parameter calibration, EDEM, JKR Contact Model, rapeseed blanket seedlings

ABSTRACT

It is difficult to accurately calculate the mutual force and seedling loss law between seedling needles and seedlings when conducting simulation analysis of cutting and transplanting rapeseed blanket seedlings with a transplanting machine due to a lack of reliable discrete element simulation parameters for rapeseed blanket seedlings. The physical and contact parameters of rapeseed blanket seedlings are calibrated in this study using the EDEM discrete element method. The Hertz Mindlin with JKR model in EDEM software was used to simulate the shear force of rapeseed blanket seedlings after conducting experiments to determine the density, shear modulus, Poisson's ratio, friction coefficient, and collision recovery coefficient between seedlings and steel materials. The surface energy parameters, recovery coefficient, static friction coefficient, and rolling friction coefficient between seedlings were used as experimental variables, with the maximum shear force of seedlings serving as the response value. Using Box Behnken's response surface optimization method, multiple regression fitting analysis was performed on the experimental results to obtain the regression model of seedling shear force, which was then optimized to obtain the parameter optimization solution for rapeseed blanket seedlings. Finally, the collision recovery coefficient was calculated to be 0.6. The ideal contact characteristics for seedlings are a static friction coefficient of 0.8, a rolling friction coefficient of 0.3, and a JKR surface energy of 12.3 J/m².

摘要

在进行油菜毯状苗移栽机切块取苗仿真分析时，由于缺乏可靠的油菜毯状苗的苗片离散元仿真参数，难以准确计算取苗秧针-苗片相互间受力和苗片损失规律。本研究基于 EDEM 离散元法对油菜毯状苗的苗片物理与接触参数进行标定。通过试验测定苗片密度、剪切模量、泊松比以及苗片-苗片、苗片-钢材料之间的摩擦系数和碰撞恢复系数，采用 EDEM 软件中的 Hertz-Mindlin with JKR 模型对油菜毯状苗的苗片进行剪切力仿真试验，以苗片间表面能参数、恢复系数、静摩擦系数、滚动摩擦系数为试验因素，以苗片最大剪切力为响应值，基于 Box-Behnken 的响应面优化方法，对试验结果进行多元回归拟合分析得到苗片剪切力的回归模型，并对回归模型进行寻优，得到油菜毯状苗苗片的参数优化解，最终确定碰撞恢复系数 0.6、静摩擦系数 0.8、滚动摩擦系数 0.3、JKR 表面能 12.3 J/m² 是苗片的最优接触参数组合。

INTRODUCTION

The rapeseed blanket seedling transplanter accurately separates seedlings from seedlings while also improving the speed and efficiency of seedling extraction through mechanized operation (Yu Gaohong et al., 2022). During the seedling-picking process, the seedling-picking mechanism splits the seedling pieces into seedling blocks, which can easily cause damage and impact planting quality. Traditional physical experiments fail to adequately determine the damage mechanism of seedling blocks during the seedling harvesting procedure. Virtual simulation is the only way to model the dynamic process of seedling particle mobility and interaction. Before employing the discrete element approach to simulate the interaction between soil-contacting components and seedlings, the simulation parameters between seedling particles must be calibrated.

In agricultural engineering, research on discrete element parameter calibration is mostly focused on soil and agricultural material particles (Zeng *et al.*, 2021; Chan *et al.*, 2021). In the field of soil discrete element parameter calibration, for example, Xiaoning He *et al.* (2024) used Hertz Mindlin and Johnson Kendall Roberts (JKR) models to calibrate the contact parameters between saline soil particles as the test factor and soil accumulation angle as the test index and conducted saline soil contact parameter calibration experiments to determine the optimal combination of saline soil contact parameters. Shaochuan Li *et al.* (2023) studied no-till soil and determined the Edinburgh Elasto Plastic Adhesion (EEPA) model as the soil contact model by obtaining the relationship between loading force and deformation through uniaxial sealing compression tests. They used the Plackett Burman test and quadratic orthogonal rotation test to establish regression equations and analyze the interaction effects. The measured values of stacking angle and strain were obtained through the stacking angle test and uniaxial sealing compression test, and the optimal solution was obtained. The simulation values and measured values under the optimal parameters were compared and verified, and it was found that the error values were less than 1%. Bin Chen *et al.* (2022) calibrated the contact parameters between soil particles using the soil angle of repose test and between soil and machinery using the soil sliding test. The Hertz Mindlin JKR contact model was used for soil particles, and the Hertz Mindlin (no slip) contact model was used for soil particles and steel components. The errors between the simulation test and the physical test were 3.94% and 3.66%, respectively, through the stacking angle test and sliding angle test. These studies mainly focus on the discrete element parameters of pure soil, often using the JKR model and soil accumulation tests for parameter calibration. However, the actual soil is complex and often contains other biomass such as straw, roots, etc. Pure soil cannot fully reflect the actual soil state. Zenghui GAO *et al.* (2022) used the Hertz Mindlin with JKR contact model for parameter calibration of wheat straw soil mixture. The stacking angle test, Plackett Burman screening method, and steepest slope test were used to determine the optimal combination range of each parameter, and the Box Behnken test was used to find the optimal solution. Shilin Zhang *et al.* (2022) selected the Hertz Mindlin with JKR Cohesion contact model for maize root and soil mixtures and developed DEM models for maize single roots (SMR) and maize root soil mixtures (MRSM) with different diameters based on calibration parameters through angle of repose experiments. In the study of agricultural materials such as seeds and straw, Guoqiang Dun *et al.* (2024) selected the Hertz Mindlin no-contact model as the simulation contact model for Chinese cabbage seeds. Physical experiments were conducted to determine the basic physical and contact parameters of Chinese cabbage seeds. Based on the results of the physical experiments, the simulation parameter range was determined. The Plackett Burman experiment was used to screen the factors that significantly affect the stacking angle from each group of experimental parameters, and the optimal range of the two factors was further determined through the steepest climbing experiment. The regression equation between the significant parameters and the stacking angle is obtained through a second-order universal rotation combination test, and the optimal parameter combination is obtained by optimizing the measured stacking angle. Min Fu *et al.* (2023) used crushed corn stover as the research object and calibrated simulation parameters using a combination of physical measurements and virtual experiments. A Hertz Mindlin with JKR Cohesion contact model was used to establish a discrete element model for crushed corn stover, and virtual stacking experiments were conducted using EDEM software. The above research indicates that by comparing the simulated test angle of repose and the actual pile-up test angle of repose through pile-up experiments to determine the discrete element parameters, it can be found that such research objects are generally flowable bulk particles, but for materials that are not easy to flow, calibration cannot be completed through pile up experiments. Scholars at home and abroad have also researched this issue, Guoyang Liu *et al.* (2021) concatenated a nonlinear viscoplastic model with a Burgers model to form a nonlinear viscoelastic plastic model, and introduced creep test curves into the model for fitting. Through verification experiments, the nonlinear model was compared with the Burgers model, and the results showed that the fitting accuracy of the nonlinear model was better than that of the Burgers model. Jiawei Xu *et al.* (2023) combined Hertz Mindlin with bonding cohesive and Hertz Mindlin cohesive contact models (reflecting the cohesiveness and structure of soft clay, respectively) to reproduce the bonding process of clay, and established numerical models for lateral compression test, cross plate shear test, and triaxial test. The deformation and stress-strain development were in good agreement with the experimental results. Syfur Rahman *et al.* (2020) developed a discrete element model for cohesive soil mixtures using random irregular particle combinations with different microbonding strengths. The microscale model parameters are determined by macroscopic characteristics obtained from laboratory compression tests and calibrated based on actual stress-strain behavior. The indirect tensile test simulation is highly consistent with the actual stress-strain behavior of soil mixtures.

Hongbin Bai et al. (2023) applied the Hertz Mindlin with bonding model to model the matrix block, and used the maximum puncture force as the evaluation index. The two-level factorial test and steepest climbing test were used to screen for significant parameters and optimal intervals. Through the Box Behnken test and optimization solution, the optimal combination of bonding parameters for the matrix block particles was obtained. Simulation verification was carried out for the optimal parameter combination, and the relative error between the simulated value and the measured value of the maximum puncture force was 1.88%. These studies provide new parameter calibration experimental methods that can determine the optimal discrete element parameters through stress-strain comparison experiments.

Therefore, based on the characteristics of rapeseed blanket seedlings, physical experiments were used to determine the basic physical parameters of rapeseed blanket seedlings, including density, shear modulus, Poisson's ratio, as well as the friction coefficient and collision recovery coefficient between seedlings and steel materials, based on the shear force test of seedlings. Using EDEM software to construct a simulation model of seedlings, with maximum shear force as the evaluation index, using Design Expert software to determine the optimal values of seedling simulation parameters, and conducting calibration experiments on seedling contact parameters, providing basic parameters for the discrete element simulation of rapeseed blanket seedlings.

MATERIALS AND METHODS

Particle modeling of seedling sheets

The rapeseed variety is Ningza 1838. The seedling substrate is spread in plastic seedling trays with a length, width, and height of 300 mm, 600 mm, and 30 mm. The rapeseed seeds are sown according to the prescribed row spacing and plant spacing to cultivate carpet-like seedlings (Figure 1a). The seedling age is 30 days, the seedling height is 90 mm, and the seedling density is 3500 plants/m². The seedling substrate mainly includes substances such as coconut coir, peat, and vermiculite. After 30 days of growth, the root system and seedling substrate interweave to form a whole, forming seedling pieces with a thickness of 20 mm. The seedling piece sample used in the experiment is the part of the seedling above the cut seedling piece (Fig.1b).



(a) Rapeseed blanket seedling

(b) Seedling slice sample

Fig. 1 - Rapeseed blanket seedling sheets

Density determination of seedling sheets

Select 10 samples of seedlings with dimensions of 30 mm × 30 mm × 20 mm, measure the mass of seedlings using a high-precision electronic scale, calculate the density of seedlings according to equation (1), and take the average value, that is, $\rho = 830 \text{ kg/m}^3$

$$\rho = \frac{m}{V} \quad (1)$$

ρ is the density of seedlings, [kg/m³]; m - mass of the seedling, [kg]; V - volume of the seedling sample, [m³].

Shear modulus determination of seedling sheets

The TJ strain-controlled three-speed electric soil direct shear apparatus (Figure 2a) produced by Nanjing Soil Instrument Factory is used for seedling shear tests. The sampling ring knife provided with the direct shear apparatus is used to vertically press into the seedlings and take out a circular cake-shaped carpet-shaped seedling sample with a thickness of 20 mm and a cross-sectional area of 30 cm². It is placed between the upper and lower boxes (Figure 2b), loaded with a 1:12 lever, and two normal loads of 400kPa and 200kPa are used. A fast-cutting method with a cutting speed of 0.8 mm/min is adopted. The shear modulus of the seedlings calculated by formula (2) is $G = 0.22 \text{ MPa}$.

$$G = \frac{\tau}{\gamma} \quad (2)$$

where G is the shear modulus, [N/m²]; τ is the shear stress, [N/m²]; γ is the shear strain, dimensionless.

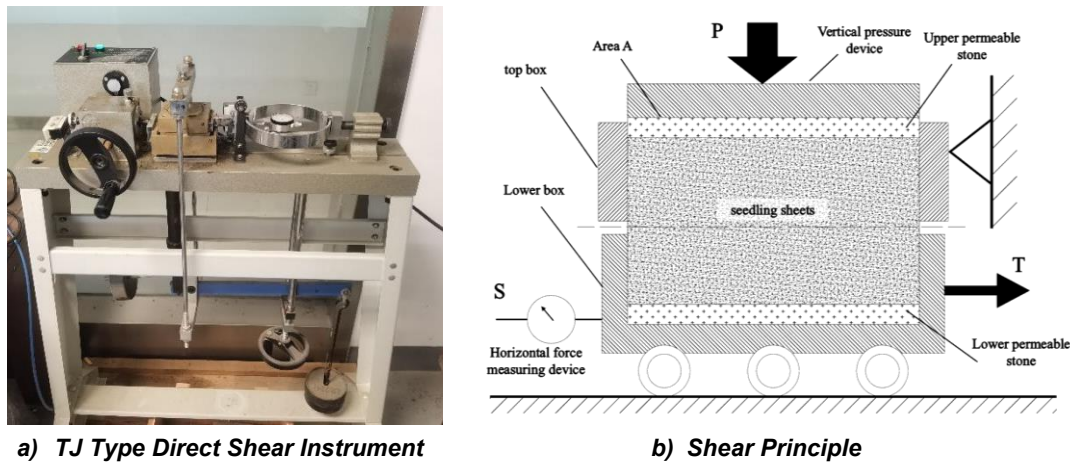


Fig. 2 - TJ type direct shearing instrument and shearing principle

Poisson's ratio of rapeseed blanket seedling sheets

Poisson's ratio refers to the ratio of lateral deformation to axial deformation of seedlings under unidirectional tension or compression and is an elastic index reflecting the lateral deformation of seedlings. During the experiment, the seedlings were made into standard cubic specimens with a side length of 20 mm, and the Poisson's ratio of the seedlings was calculated using formula (3) to obtain $\mu=0.3034$.

$$\mu = \left| \frac{\delta_1}{\delta_2} \right| = \frac{W_1 - W_2}{L_1 - L_2} \quad (3)$$

where μ is Poisson's ratio, δ_1 is the lateral deformation amount, [mm]; δ_2 is the axial deformation amount, [mm]; W_1 and W_2 are the transverse dimensions before and after compression, [mm]; L_1 and L_2 are the axial dimensions of the seedlings before and after compression, [mm].

Friction coefficient

The static friction coefficient is the ratio of the maximum static friction force experienced by an object to the normal pressure. The inclined sliding method is used to measure the static friction coefficient between seedlings and steel plates, as well as between seedlings (Figure 3a). During the experiment, the stainless steel plate is adjusted to a horizontal state. When measuring the static friction coefficient between the seedling and the steel, the 20 mm cube seedling sample is directly placed on the stainless steel plate. When measuring the static friction coefficient between seedlings, lay the seedlings with a length x width of 580 mm x 280 mm flat on a stainless steel plate, and place a 20 mm cube seedling sample on the seedlings. Place the electronic angle meter on a stainless steel plate for easy observation of the angle degree. Slowly lift one end of the stainless steel plate to increase the tilt angle. When the seedling sample starts to slide down the slope, stop and record the angle α displayed on the electronic protractor. Apply formula (4) to calculate the static friction coefficient.

$$f_1 = \tan \alpha \quad (4)$$

where f_1 is the static friction coefficient; α is the critical angle of static friction, [$^\circ$].

The rolling friction coefficient between seedlings and steel plates, as well as between seedlings, was measured using the inclined rolling method (Figure 3b). In two experiments, seedlings were made into 20 mm diameter spherical specimens and released at zero initial velocity on an inclined panel with an inclination angle of $\beta=15^\circ$ and a vertical height of $H_2=80$ mm.

The spherical specimens rolled downwards along the inclined panel for a distance S . Due to rolling friction, the spherical specimens finally rolled a distance L_2 on the horizontal panel and stopped. Assuming that the spherical specimens were ideal spheres, they were only affected by rolling friction during pure rolling, and the rolling friction coefficient was calculated according to equation (5).

$$f_2 = \frac{S \sin \beta}{S \cos \beta + L_2} \quad (5)$$

where:

f_2 is the rolling friction coefficient;

β is the angle set for the stainless steel plate, [$^\circ$];

L_2 is the horizontal rolling distance of the spherical sample, [mm].

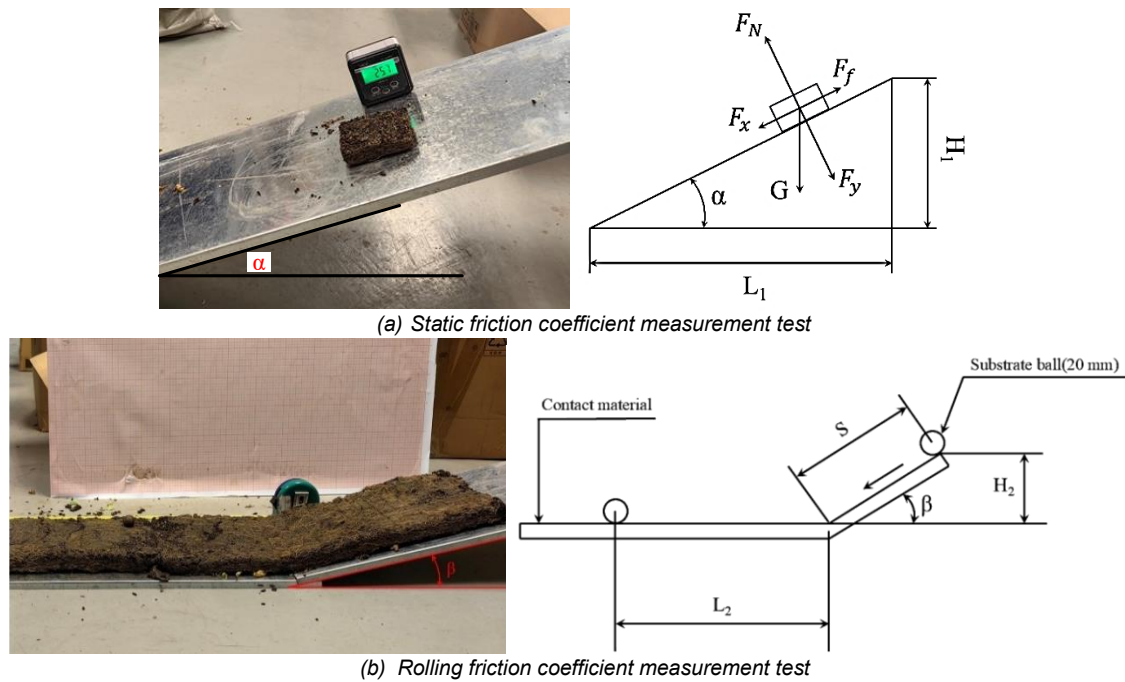


Fig. 3 - Friction coefficient measurement test

The average static friction coefficient between the seedlings and the steel plate was calculated to be 0.441, and the rolling friction coefficient was 0.0621. The average static friction coefficient between seedlings is 1.0312, and the rolling friction coefficient is 0.4223.

Collision recovery coefficient

As shown in Figure 4, the collision recovery coefficients between seedlings and seedlings, as well as between seedlings and stainless steel plates, were measured using the free fall collision method. During the experiment, a 20 mm diameter spherical sample was released at a height of $H=250$ mm from the contact bottom surface. The entire release collision process was recorded by a high-speed camera. The spherical sample bounced back when it hit the contact material (seedling or stainless steel plate), and the highest rebound height h was recorded. The collision recovery coefficient e_x is the ratio of the normal instantaneous separation velocity v_1 and instantaneous contact velocity v_0 at the collision contact point before and after the collision between the spherical sample and the contact material, that is, the ratio of the maximum collision rebound height h to the initial falling height H , calculated by formula (6).

$$e_x = \frac{v_1}{v_0} = \frac{\sqrt{2gh}}{\sqrt{2gH}} = \sqrt{\frac{h}{H}} \quad (6)$$

where e_x is the collision recovery coefficient; v_1 is the instantaneous normal velocity of the spherical specimen before collision, [mm/s]; v_0 is the instantaneous normal velocity of the spherical specimen after collision, [mm/s]; h is the initial release height of the spherical sample, [mm]; H is the initial release height of the spherical sample, [mm].

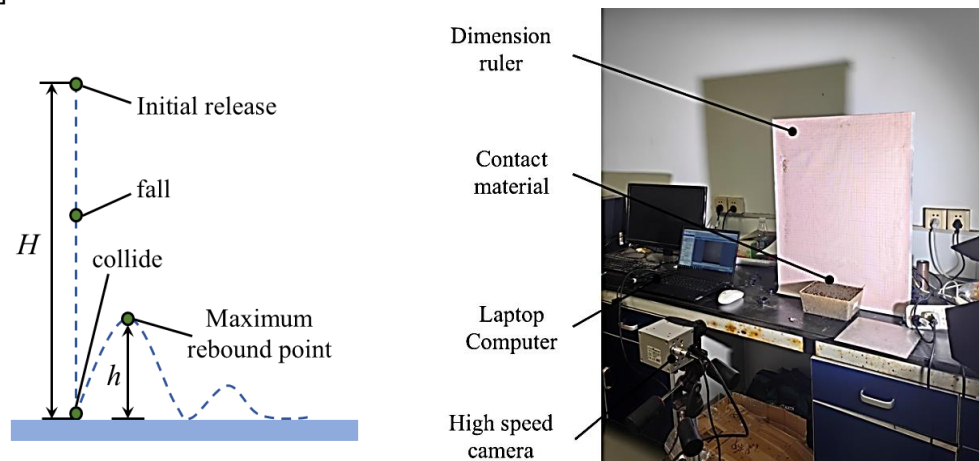


Fig. 4 - Collision Recovery Coefficient Measurement Test

Record the height before deployment and the height of the highest point after collision through high-speed photography, repeat each experiment 5 times, calculate the collision recovery coefficient using equation (6), and take the average of the results. The recovery coefficient for collision between seedlings and stainless steel plates is 0.728, and the recovery coefficient for collision between seedlings is 0.4129.

Determination of particle contact models for seedling sheets

The Hertz Mindlin with JKR model is a cohesive contact model that combines Hertz contact theory with JKR theory to consider the influence of interparticle bonding forces on particle motion. It is suitable for simulating materials with significant bonding and agglomeration between particles, such as crops and soil (Sun Jingbin et al, 2022; Wu Tao et al, 2017; Tian Xinliang et al, 2021). For the large adhesion force between the seedlings of rapeseed blanket-like seedlings, this paper selects the Hertz Mindlin with the JKR model to simulate the seedlings and calibrate the contact model parameters accordingly. When simulating wet particles using the Hertz Mindlin with JKR contact model, the force required to separate two particles depends on the liquid surface tension γ_s and wetting angle, as shown in equation (7).

$$F_p = -2\pi\gamma_s\cos(\theta)\sqrt{R_iR_j} \quad (7)$$

where F_p is the force required to separate two particles, [N]; θ is the contact angle, [°]; R is the particle radius, [mm]. Equivalent this force to the maximum cohesive force of JKR $F_p = -\frac{3}{2}\pi\gamma R^*$, where γ is the surface energy and R^* is the equivalent radius. If EDEM particles are not scaled proportionally, parameter estimation of JKR surface energy can be performed.

Seedling sheets calibration test

The JKR contact parameters (coefficient of elastic recovery, coefficient of static friction, coefficient of kinetic friction, and JKR surface energy) between seedling particles were used as testing factors, and the maximum shear force was used as the testing indicator for seedling particle contact parameter testing. As shown in Figure 5, 5 seedling specimens with dimensions of 150 mm x 100 mm x 20 mm were taken and placed on a universal mechanical testing machine. The specimens were vertically cut with a cutting blade held in place, and the average maximum shear force was obtained as 35 N.



Fig. 5 - Seedling cutting test

The test level was set based on the values of the recovery coefficient, static friction coefficient, and rolling friction coefficient of the seedlings obtained from the measurement (Table 1). The surface energy of JKR was determined according to the reference literature (Gao et al., 2022; L. Yang et al., 2024; Q. Yang et al., 2023), surface energy was set as reference values at levels of 5 J/m², 10 J/m², and 15 J/m².

Table 1

Factors and Levels of Shear Force Simulation Test				
code	JKR surface energy A/ J/m ²	Recovery coefficient B	Static friction coefficient C	Rolling friction coefficient D
-1	5	0.3	0.4	0.1
0	10	0.6	0.8	0.5
1	15	0.9	1.2	0.9

RESULTS

Simulation calibration test

The simulation model of seedling cutting is shown in Figure (6). The cutting blade used in the experiment is made of stainless steel material, and the material properties refer to the literature (Zhu Yinghao *et al.*, 2020). The density is 7.85 g/cm³, Poisson's ratio is 0.3, and the shear modulus is 79000MPa. By using EDEM software to construct the particle structure of seedlings, and following the Box Behnken four-factor three-level experimental design method, an experimental plan was developed using the factor levels listed in Table 1 using Design Expert 13.0 software. Vertical cutting simulation experiments of seedlings were conducted based on the experimental plan. To avoid calculation errors each time, each test group was repeated three times and the average value was taken as the test result. After determining the test results, determine the difference between the test results and the actual shear force of the seedlings. The test plan and its results are shown in Table 2.

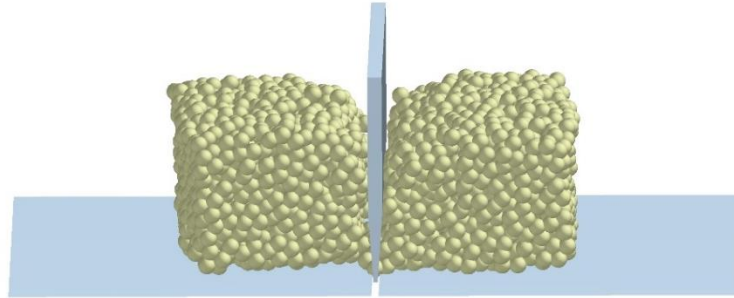


Fig. 6 - Simulation experiment of seedling cutting

Table 2

Design and Results of Shear Force Simulation Experiment on Rapeseed Blanket Seedlings Matrix

Test number	JKR surface energy A/ J/m ²	Recovery coefficient B	Static friction coefficient C	Rolling friction coefficient D	Shear force Y/N
1	10	0.3	0.8	0.1	10.17
2	10	0.3	1.2	0.5	12.97
3	10	0.6	1.2	0.1	9.89
4	5	0.9	0.8	0.5	34.46
5	10	0.9	0.8	0.1	9.62
6	10	0.6	0.4	0.1	30.55
7	5	0.6	0.4	0.5	34.93
8	10	0.6	0.8	0.5	71.73
9	15	0.9	0.8	0.5	35.2
10	10	0.3	0.8	0.9	10.19
11	10	0.3	0.4	0.5	15.12
12	10	0.6	1.2	0.9	17.93
13	10	0.9	0.8	0.9	13.03
14	10	0.9	1.2	0.5	10.39
15	5	0.6	1.2	0.5	27.37
16	5	0.3	0.8	0.5	25.56
17	10	0.6	0.8	0.5	69.13
18	15	0.6	0.4	0.5	46.6
19	15	0.6	0.8	0.9	42.3
20	5	0.6	0.8	0.1	33.92
21	15	0.6	1.2	0.5	40.4
22	15	0.6	0.8	0.1	39.4
23	10	0.6	0.8	0.5	71.72
24	10	0.6	0.4	0.9	21.57
25	15	0.3	0.8	0.5	36.7
26	10	0.6	0.8	0.5	69.69
27	5	0.6	0.8	0.9	24.55
28	10	0.9	0.4	0.5	27.03
29	10	0.6	0.8	0.5	68.43

Result analysis

According to the experimental factor levels in Table 2, shear force simulation experiments were conducted, and regression analysis of variance was performed on the experimental results. The results are shown in Table 3. Through multiple regression analysis of the experimental data, the shear force regression model for rapeseed blanket seedling substrate was obtained as follows:

$$Y = 70.14 + 4.98A + 1.58B - 4.74C - 0.3317D + 3.07AD - 3.62BC + 4.26CD - 7.81A^2 - 30.43B^2 - 23.64C^2 - 27.59D^2 \quad (8)$$

Among them, coefficient of determination $R^2 = 0.9895$ and correction coefficient of determination $Adj - R^2 = 0.9827$.

According to Table 3, the P-value of the model is less than 0.0001, indicating that the model is highly significant and can be used to predict the maximum shear force between matrices. Within the reference range of experimental factors, A, B, and C have a significant impact on the maximum shear force, with C being extremely significant. The rolling friction coefficient D has no significant impact on the maximum shear force, but D^2 is significant. The interaction between AD, BC, and CD is significant.

Table 3

Source	Sum of Squares	df	Mean Square	F-value	p-value
Model	11517.43	14	822.67	125.78	< 0.0001
A	298.1	1	298.1	45.58	< 0.0001
B	30.15	1	30.15	4.61	0.0498
C	269.33	1	269.33	41.18	< 0.0001
D	1.32	1	1.32	0.2018	0.6601
AB	27.04	1	27.04	4.13	0.0614
AC	0.4624	1	0.4624	0.0707	0.7942
AD	37.64	1	37.64	5.75	0.0309
BC	52.49	1	52.49	8.03	0.0133
BD	2.87	1	2.87	0.4393	0.5182
CD	72.42	1	72.42	11.07	0.005
A^2	395.31	1	395.31	60.44	< 0.0001
B^2	6004.58	1	6004.58	918.06	< 0.0001
C^2	3623.95	1	3623.95	554.08	< 0.0001
D^2	4937.72	1	4937.72	754.94	< 0.0001
Residual	91.57	14	6.54		
Lack of Fit	82.4	10	8.24	3.59	0.1146
Pure Error	9.17	4	2.29		
Cor Total	11608.99	28			

To explore the interaction between the four testing factors and the response values, according to Table 3, the interaction between AD, BC, and CD has a significant impact on the maximum shear force and response surface and contour distribution of seedlings, as shown in Figure 7. The curvature of the response surface indicates that the order of the influence of interaction terms on the maximum shear force of seedlings is $CD > BC > AD$. As shown in Figure 7 (a), the maximum shear force of seedlings increases first and then decreases with the increase of dynamic friction coefficient and collision recovery coefficient. The maximum shear force of seedlings changes with the simultaneous increase of both, and the impact of the collision recovery coefficient on the maximum shear force of seedlings is minimal. From Figure 7 (b), it can be seen that the maximum shear force of seedlings increases first and then decreases with the increase of static friction coefficient and collision recovery coefficient, and the two interact with each other. The maximum shear force of seedlings changes with the simultaneous increase of both. Figure 7 (c) shows that the maximum shear force of seedlings increases first and then decreases with the increase of static friction coefficient and dynamic friction coefficient, and the two interact with each other. The maximum shear force of seedlings changes with the simultaneous increase of both.

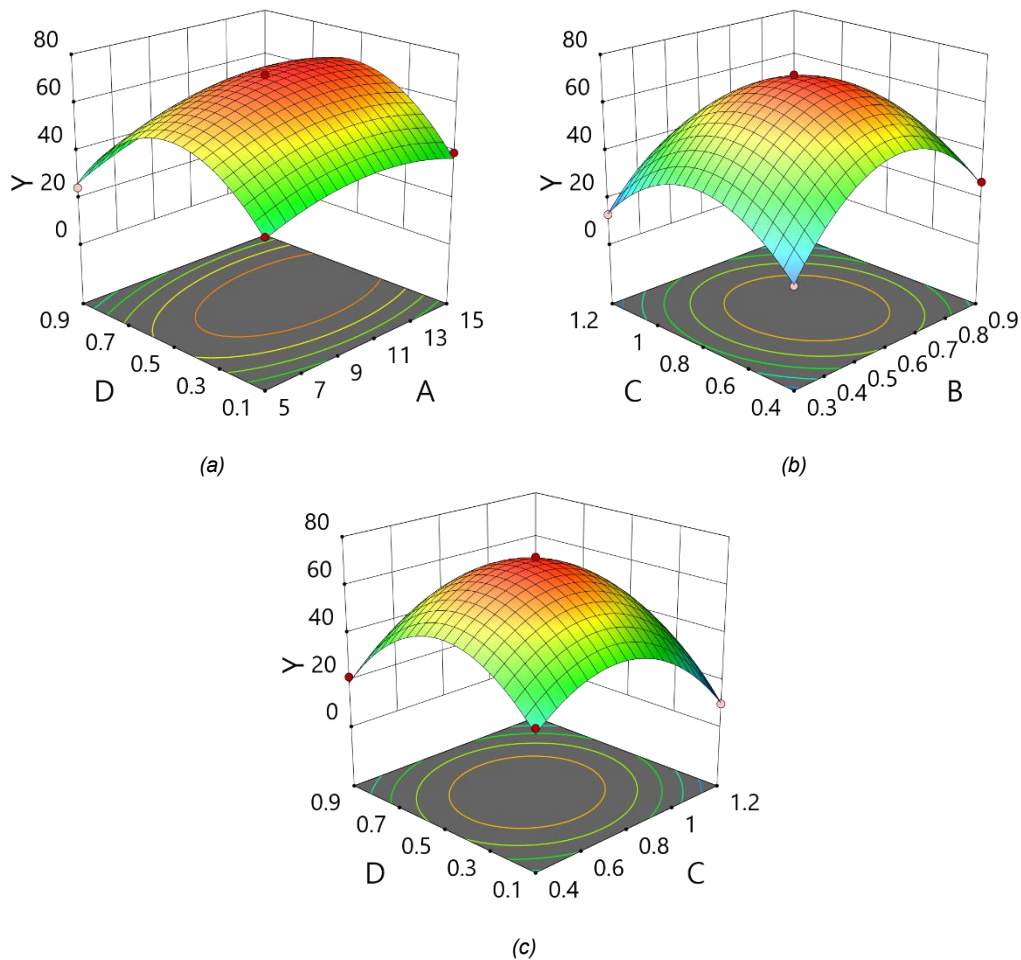


Fig. 7 - Maximum Shear Force Interaction of Seedlings
 (a) AD Effect on maximum shear stress of matrix; (b) BC Effect on maximum shear stress of matrix;
 (c) CD Effect on maximum shear stress of matrix

Parameter optimization and validation

The maximum shear force physical experiment measured that the maximum shear force of the matrix sample under shear was 35 N. Through the optimization module of Design Expert software, the regression model was optimized with the maximum shear force of the matrix sample as the objective, and an optimized solution similar to the maximum shear force of the matrix sample was selected. The simulation results show that when the surface energy of JKR between matrices is 12.3 J/m², the recovery coefficient is 0.6, the static friction coefficient is 0.8, and the rolling friction coefficient is 0.3, the simulation result is 36.1 N, which is close to the average value of 35 N in physical experiments, with a relative error of 3.14% (Figure 8).

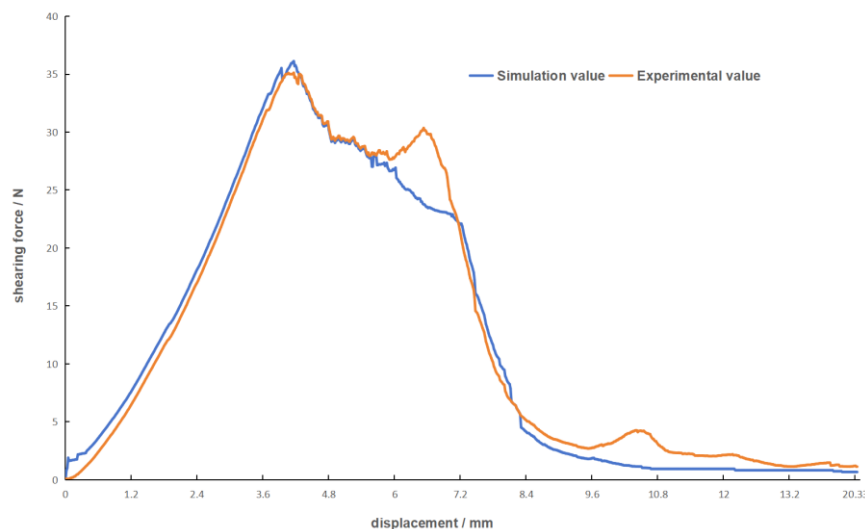


Fig. 8 - Comparison of Shear Force Test and Simulation Results of Seedlings

CONCLUSIONS

This study measured the physical parameters of rapeseed blanket seedlings and obtained a seedling density of 830 kg/m^3 , a shear modulus of $G=0.22 \text{ MPa}$, a Poisson's ratio of $\mu=0.3034$, a static friction coefficient of 0.441 between seedlings and steel plates, a dynamic friction coefficient of 0.0621 between seedlings and steel plates, and a collision recovery coefficient of 0.728 between seedlings and steel plates. Based on the discrete element method, Hertz Mindlin with the JKR model was used to simulate the substrate suitable for planting rapeseed blanket seedlings. The simulation parameters of the contact model between substrate particles were calibrated through maximum shear force simulation experiments and compared with physical experiments to obtain the maximum shear force regression equation. The parameters of the contact model between seedlings were obtained using the response surface optimization method, which were: JKR surface energy of 12.3 J/m^2 , recovery coefficient of 0.6, static friction coefficient of 0.8, and rolling friction coefficient of 0.3. When conducting relevant discrete element simulation experiments on the substrate suitable for planting rapeseed blanket seedlings, corresponding parameter values can be referred to.

This study has a certain role in the construction of a discrete element model for rapeseed blanket seedlings and the analysis of the interaction mechanism between seedlings and agricultural machinery seedling components, especially in the study of the mechanical properties of seedling particles and the changes in the physical properties of soil components in contact with seedlings during agricultural machinery operations such as transplanting and covering. However, this study mainly provides a method for constructing a discrete element particle contact model and parameter calibration of rapeseed blanket seedlings. The model parameters have complexity and variability under different seedling conditions and need to be reconstructed and calibrated based on factors such as substrate type, particle size composition, and moisture content.

ACKNOWLEDGEMENT

This research was supported by the China Postdoctoral Science Foundation (2023M740866); the National Key Research and Development Program of China (2023YFD2001001); the Jiangsu Province Modern Agricultural Machinery Equipment and Technology Demonstration and Promotion Project of China (NJ2024-01); the Jiangxi Province Agricultural Machinery Equipment, Manufacturing, Popularization and Application Integration Pilot Project (YCTY202403-02-02).

REFERENCES

- [1] Bai H., Li X., Zeng F., Su Q., Cui J., Wang J., Zhang Y. (2023). Calibration and experiments of the simulation bonding parameters for plug seedling substrate block (穴盘苗基质块仿真粘结参数标定与试验), *INMATEH Agricultural Engineering*, Vol. 69, no.1, pp.617–625, Bucharest/Romania. DOI: <https://doi.org/10.35633/inmateh-69-59>
- [2] Chen B., Liu Y., Yu Q., Chen X., Miao Y., He Y., Chen J., Zhang J. (2022). Calibration of soil discrete element contact parameter in rhizome medicinal materials planting area in hilly region (丘陵山地根茎类中药材种植区土壤离散元参数标定), *INMATEH Agricultural Engineering*, Vol. 68, no.3, pp.521–532, Bucharest/Romania. DOI: <https://doi.org/10.35633/inmateh-68-51>
- [3] Chan L., Mou X., Pong Z. (2021). Application of Discrete Element Method in Agricultural Engineering (离散元法在农业工程中的应用). *Agricultural Engineering*, Vol. 11, no.8, pp.29-34, Beijing/China.
- [4] Dun G., Zhang C., Ji X., Meng Q., Sheng Q., Wang L. (2024). Simulation parameter calibration and test of pak choi seeds based on discrete element method (基于离散元的小白菜种子仿真参数标定与试验), *INMATEH Agricultural Engineering*, Vol. 73, no.2, pp.391–405, Bucharest/Romania. DOI: <https://doi.org/10.35633/inmateh-73-33>
- [5] Fu M., Chen X., Gao Z., Wang C., Xu B., Hao Y. (2023). Parameters calibration of discrete element model for crushed corn stalks (碎玉米秸秆离散元模型参数标定), *INMATEH Agricultural Engineering*, Vol. 69, no.1, pp.399–408, Bucharest/Romania. DOI: <https://doi.org/10.35633/inmateh-69-37>
- [6] Gao Z., Shang S., Xu N., Wang D. (2022). Parameter calibration of discrete element simulation model of wheat straw-soil mixture in Huang Huai Hai production area (黄淮海产区小麦秸秆-土壤混合物的离散元仿真模型参数标定), *INMATEH Agricultural Engineering*, Vol. 66, no.1, pp.201–210, Bucharest/Romania. DOI: <https://doi.org/10.35633/inmateh-66-20>

- [7] He X., Ma S., Liu Z., Wang D., Shang S., Li G., Li H. (2024). Calibration and testing of saline soil parameters based on EDEM discrete element methodology (基于 EDEM 离散元方法的盐碱土壤参数标定与测试), *INMATEH Agricultural Engineering*, Vol. 73, no.2, pp.822–833, Bucharest/Romania. DOI: <https://doi.org/10.35633/inmateh-73-69>
- [8] Li S., Diao P., Zhao Y., Miao H., Li X., Zhao H. (2023). Calibration of discrete element parameter of soil in high-speed tillage (高速耕作条件下土壤离散元参数标定), *INMATEH Agricultural Engineering*, Vol. 71, no.3, pp.248–258, Bucharest/Romania. DOI: <https://doi.org/10.35633/inmateh-71-21>
- [9] Liu G., Xia J., Zheng K., Cheng J., Jiang L., Guo L. (2021). Creep properties and prediction model of paddy soil under compression (水稻土受压蠕变特性及预测模型构建), *INMATEH Agricultural Engineering*, Vol. 65, no.3, pp.441–451, Bucharest/Romania. DOI: <https://doi.org/10.356.33/inmateh-65-46>
- [10] Rahman S., Khattak M., Adhikari B., Adhikari S. (2020). Discrete element modeling of bonded soil mixtures under uniaxial compression and indirect tension test. *Transportation Geotechnics*, Vol 26, Netherlands. DOI: <https://doi.org/10.1016/j.trgeo.2020.100438>
- [11] Sun J., Liu Q., Yang F., Liu Z., Wang Z. (2022). Calibration of Discrete Element Simulation Parameters of Sloping Soil on Loess Plateau and Its Interaction with Rotary Tillage Components (黄土高原坡地土壤与旋耕部件交互离散元仿真参数标定), *Transactions of the Chinese Society for Agricultural Machinery*, Vol 53, no.1, pp.63–73, Beijing/China. DOI: <https://doi.org/10.6041/j.issn.1000-1298.2022.01.007>
- [12] Tian X., Cong X., Qi J., Guo H., Li M., Fan X. (2021). Parameter Calibration of Discrete Element Model for Corn Straw-Soil Mixture in Black Soil Areas (黑土区玉米秸秆 – 土壤混料离散元模型参数标定), *Transactions of the Chinese Society for Agricultural Machinery*, Vol 52, no.10, pp.100-108,242, Beijing/China. DOI: <https://doi.org/10.6041/j.issn.1000-1298.2021.10.010>
- [13] Wu T., Huang W., Chen X., Ma X., Han Z., Pan T. (2017). Calibration of discrete element model parameters for cohesive soil considering the cohesion between particles (考虑颗粒间黏结力的黏性土壤离散元模型参数标定), *Journal of South China Agricultural University*, Vol 38, no.3, pp.93–98, Guangdong/China. DOI: <https://doi.org/10.7671/j.issn.1001-411X.2017.03.015>
- [14] Xu J., Ye J., Sun J., Bian X. (2023). Discrete-element method modeling of structural clay. *Proceedings of the Institution of Civil Engineers-Geotechnical Engineering*, Vol 177, no.6, pp.717–732, London/England. DOI: <https://doi.org/10.1680/jgeen.22.00224>
- [15] Yang L., Li J., Lai Q., Zhao L., Li J., Zeng R., Zhang Z. (2024). Discrete element contact model and parameter calibration for clayey soil particles in the Southwest hill and mountain region. *Journal of Terramechanics*, Vol 111, pp.73–87, Netherlands. DOI: <https://doi.org/10.1016/j.jterra.2023.10.002>
- [16] Yang Q., Shi L., Shi A., He M., Zhao X., Zhang L., Addy M. (2023). Determination of key soil characteristic parameters using angle of repose and direct shear stress test. *International Journal of Agricultural and Biological Engineering*, Vol 16, no.3, pp.143–150, Beijing/China. DOI: <https://doi.org/10.25165/j.ijabe.20231603.6293>
- [17] Yu G., Wang L., Sun L., Zhao X., Ye B. (2022). Advancement of Mechanized Transplanting Technology and Equipments for Field Crops. *Transactions of the Chinese Society for Agricultural Machinery*, Vol 53, no.9, pp.1–20, Beijing/China. DOI: <https://doi.org/10.6041/j.issn.1000-1298.2022.09.001>
- [18] Zhang S., Yang F., Dong J., Chen X., Liu Y., Mi G., Wang T., Jia X., Huang Y., Wang X. (2022). Calibration of Discrete Element Parameters of Maize Root and Its Mixture with Soil. *Processes*, Vol 10, no.11, Switzerland. DOI: <https://doi.org/10.3390/pr10112433>
- [19] Zeng Z., Ma X., Cao X., Li Z., Wang X. (2021). Critical Review of Applications of Discrete Element Method in Agricultural Engineering (离散元法在农业工程研究中的应用现状和展望). *Transactions of the Chinese Society for Agricultural Machinery*, Vol 52, no.4, pp.1-20, Beijing/China. DOI: <https://doi.org/10.6041/j.issn.1000-1298.2021.04.001>
- [20] Zhu Y., Xia J., Zeng R., Zheng K., Du J., Liu Z. (2020). Prediction Model of Rotary Tillage Power Consumption in Paddy Stubble Field Based on Discrete Element Method (基于离散元的稻板田旋耕功耗预测模型研究), *Transactions of the Chinese Society for Agricultural Machinery*, Vol 51, no.10, pp.42–50, Beijing/China. DOI: <https://doi.org/10.6041/j.issn.1000-1298.2020.10.006>